

## Supplementary Information

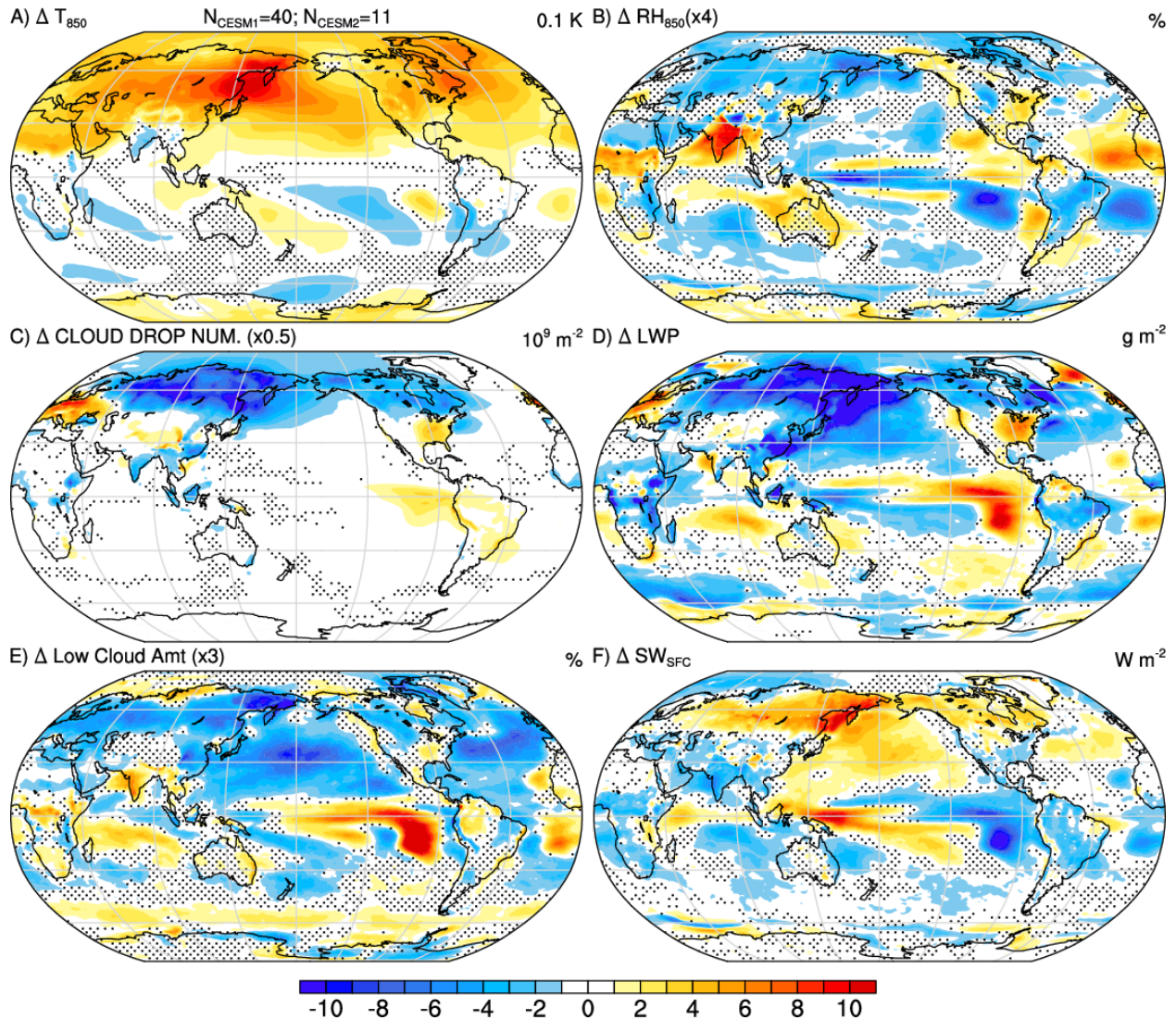
### Spurious Late Historical-Era Warming in CESM2 Driven by Prescribed Biomass Burning Emissions

J. T. Fasullo<sup>\*1,2</sup>, Jean-Francois Lamarque<sup>1</sup>, Cecile Hannay<sup>1</sup>, Nan Rosenbloom<sup>1</sup>, Simone Tilmes<sup>1</sup>,  
Patricia DeRepentigny<sup>2</sup>, Alexandra Jahn<sup>2</sup>, and Clara Deser<sup>1</sup>

#### Contents of this file Figures S1 to S2 and descriptive text.

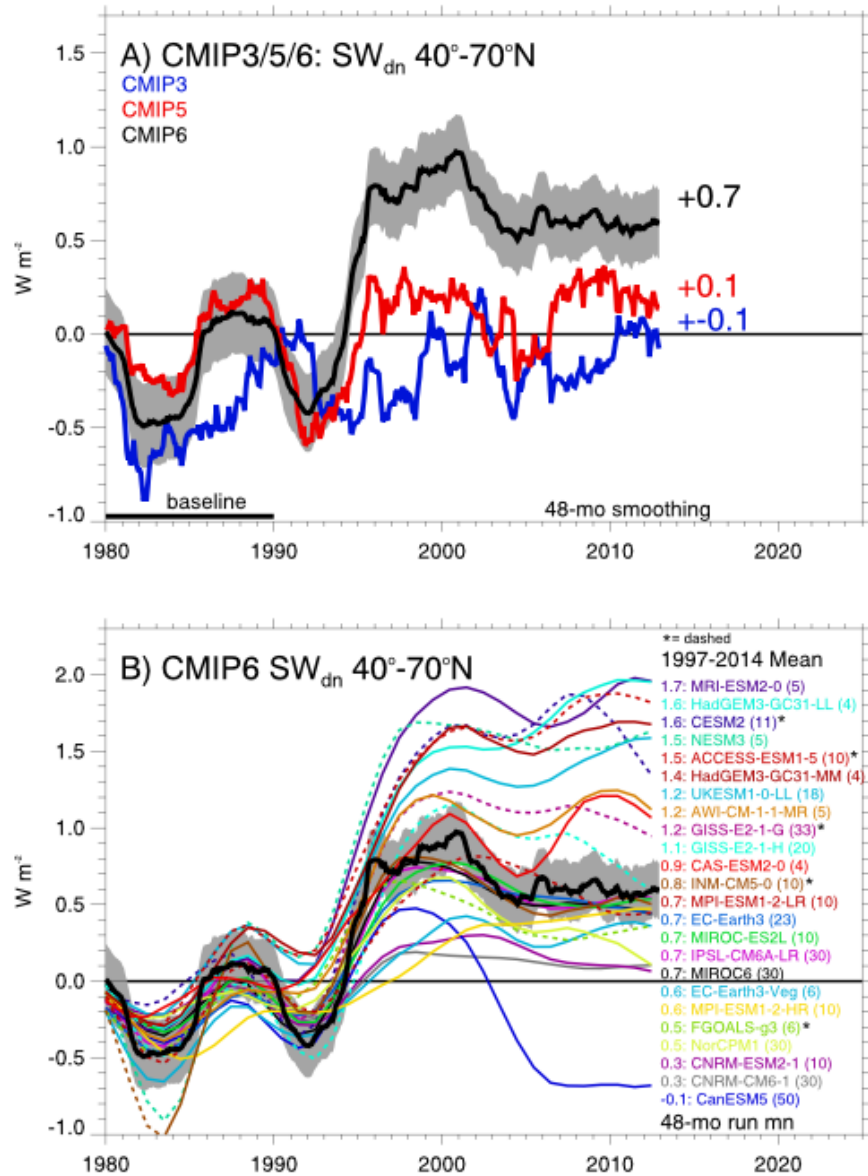
The spatial structure of anomalous warming of CESM2 during the GFED era relative to that in CESM1, estimated by the inter-model differences in the changes between 20-yr intervals, 1995-2014 and 1970-1989, is characterized by disproportionately strong warming at northern mid and high latitudes. The regions of disproportionate warming (Figure S1a) are located over, and to the east of, eastern continental boundaries in Eurasia and North America. Contrasting changes in 850 hPa relative humidity (RH; Figure S1b), where low clouds are common at high latitudes, are more spatially complex than for temperature and likely reflect both dynamical responses to BB emissions and contrasts in model physics. Yet systematically stronger decreases are generally evident in regions of disproportionate warming (shown below). Strongly coherent with the BOAS and BONA regions are disproportionate reductions in cloud drop number in CESM2 (Figure S1c), reductions that are much larger than model differences elsewhere on the globe. Relative cloud liquid water path (LWP) changes (Figure S1d) are also negative in CESM2, both in regions coherent with cloud drop number changes and to their east, suggesting a potential role for advection of cloud anomalies downstream from the BOAS and BONA regions. Spatially correlated to reductions in LWP are reductions in low cloud amount (Figure S1e) and increases

22 in  $SW_{sfc}$  (Figure S1f). Considered in tandem, these diagnostics provide a mechanistic perspective  
 23 on the drivers of disproportionate high latitude warming in CESM2 during the GFED era  
 24 whereby the increased variability in emissions drive net reductions in RH and cloud drop number  
 25 that decrease low cloud amount and thickness, and increase  $SW_{sfc}$  and warming, both locally and  
 26 downstream from the BOAS and BONA emission regions.



27  
 28 **Figure S1.** Differences in spatial structure of late historical-era changes between CESM2 and  
 29 CESM1. Shown are CESM2 minus CESM1 differences in changes (1995-2014 minus  
 30 1970-1989) in (a) temperature and (b) relative humidity at 850 hPa, vertically integrated

31 cloud droplet number (c) and liquid water path (d), low cloud amount (e), and net surface  
 32 shortwave flux (f). Regions where the difference in changes is less than twice the  
 33 ensemble standard error are stippled. Note that scaling is applied to some fields (see  
 34 panel titles).



35  
 36 **Figure S2.** Evidence for analogous sensitivity to BB in other CMIP6 simulations. Ensemble  
 37 mean historical-era evolution of anomalous downwelling solar radiation from 40°N-70°N

38 for (a) all simulation members submitted to the CMIP3 (blue), CMIP5 (red), and CMIP6  
39 (black) archives, and (b) by model submitted simulations to CMIP6 for which at least 4  
40 historical-era members are available. The standard deviation range across CMIP6  
41 members is shown (grey) and the average from 1980-1989 was used to baseline the  
42 timeseries. The ensemble-mean anomalies for 1997-2014 are shown with model names  
43 and number of ensemble members (parenthesis). In (a), CMIP3 and CMIP5 members  
44 have been extended through 2014 with SRES-a1b and RCP85, respectively.

45